

Induction of Smectic Layering in Nematic Liquid Crystals Using Immiscible Components. 5. Laterally Attached Side-Chain Liquid Crystalline Poly(norbornene)s and Their Low Molar Mass Model Compounds with Short Fluorocarbon Segments

Aaron C. Small and Coleen Pugh*

Department of Polymer Science, Maurice Morton Institute of Polymer Science, The University of Akron, Akron, Ohio 44325-3909

Received July 27, 2001; Revised Manuscript Received November 12, 2001

ABSTRACT: 5-[[2',5'-Bis[(4'-*n*-(perfluoroalkyl)alkoxy)benzoyl]oxy]benzyl]oxy]carbonyl]bicyclo[2.2.1]hept-2-enes with short fluorocarbon segments were polymerized by ring-opening metathesis polymerization in THF at room temperature using Mo(CHCMe₂Ph)(N-2,6-*i*-Pr₂Ph)(O*t*Bu)₂ as the initiator. Although hydrocarbon and fluorocarbon segments as short as three methylenic units each induce smectic layering in the corresponding 2,5-bis[[4'-(*n*-(perfluoroalkyl)alkoxy)benzoyl]oxy]toluene model compounds, the polymers require at least eight and three, or five and four methylenic units in the hydrocarbon and fluorocarbon segments, respectively, to organize into smectic layers; polymers with shorter hydrocarbon and/or fluorocarbon segments are nematic.

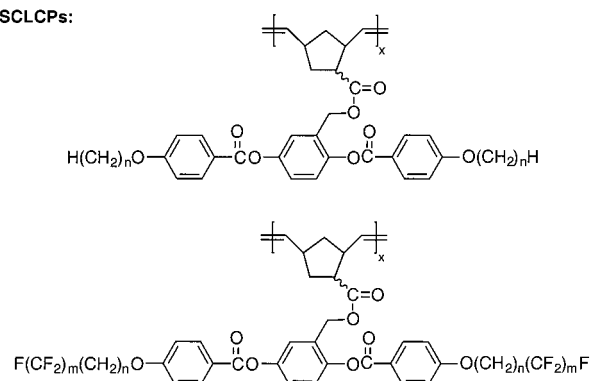
Introduction

The chemical structure of the mesogen is the primary factor dictating which phase(s) a liquid crystal forms. For example, liquid crystals based on phenyl benzoate mesogens tend to form nematic (n) mesophases.¹ However, few tools have been developed for converting the type of liquid crystalline phase exhibited by a given chemical structure, despite the discovery² of liquid crystals in 1888. One such concept is that lateral substitution of the mesogen can be used to convert smectic mesophases into nematic mesophases.³ We recently established a second concept by demonstrating that both nematic low molar mass liquid crystals (LMMLCs) and laterally attached side-chain liquid crystalline polynorbornenes with 1,4-bis[(4'-*n*-alkoxybenzoyl)oxy]benzene mesogens can be forced to order into smectic layers by terminating their *n*-alkoxy substituents (*n* = 4–6, 8 methylenic units) with immiscible fluorocarbon segments (*m* = 6–8 perfluoromethylenic units) (Scheme 1);⁴ siloxane segments are also effective although they are both flexible and much less incompatible with hydrocarbons than fluorocarbons are.⁵

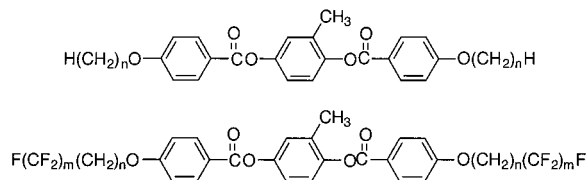
To induce smectic layering, we chose hydrocarbon and fluorocarbon segments that were long enough to microphase separate according to the microphase-separated lamellar structures formed by diblock H(CH₂)_{*n*}(CF₂)_{*m*}F and triblock H(CF₂)_{*m*}(CH₂)_{*n*}(CF₂)_{*m*}F molecules with 4 ≤ *n* ≤ 14 and *m* ≥ 6.⁶ Microsegregation of the hydrocarbon and fluorocarbon segments of 2,5-bis[(4'-*n*-(perfluoroheptyl)octyloxy)benzoyl]oxy]toluene is apparently so strong that neither lateral *n*-alkanoyl nor bulky alkanoyl or benzoate substituents disrupt the smectic layering.⁷ This paper investigates the minimum lengths of the hydrocarbon and fluorocarbon segments necessary for inducing smectic mesomorphism in the same side-chain liquid crystalline polymers (SCLCPs) and model compounds. As exemplified in Scheme 1, we have found that appropriate model compounds for laterally attached

Scheme 1. Side-Chain Liquid Crystalline Polynorbornenes and the Corresponding Model Compounds with 2,5-Bis[(4'-*n*-(perfluoroalkyl)alkoxy)benzoyl]oxy]benzene Mesogens and Their Hydrocarbon Analogues

SCLCPs:



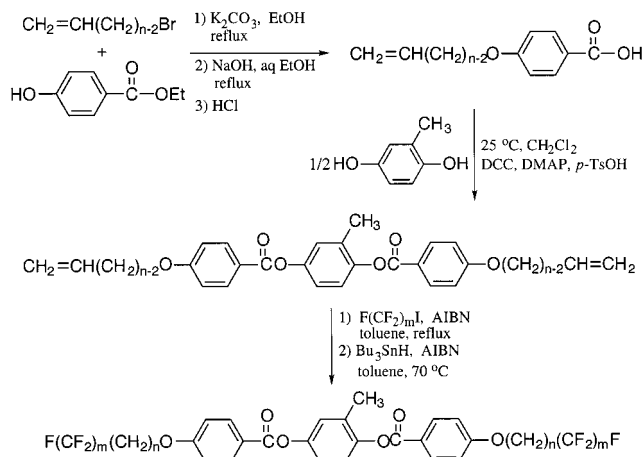
Model Compounds:



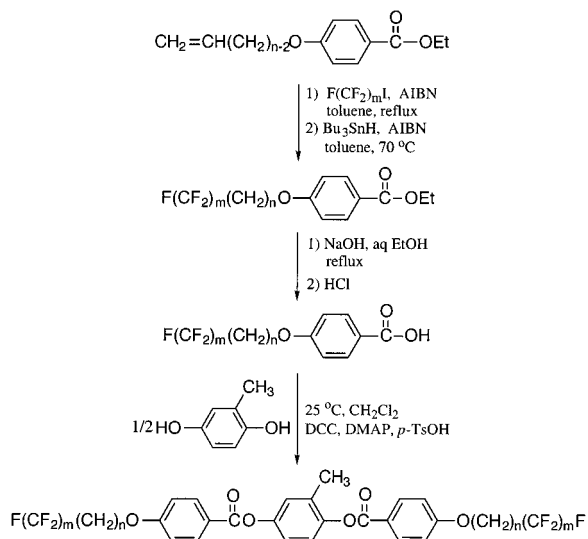
SCLCPs are based on identical mesogens with the same terminal substituents but with a lateral substituent that mimics both the chemical structure and length of the spacer.^{4,5,8} We consider the laterally attached SCLCPs to be the most challenging system possible for inducing smectic mesophases because both the molecular architecture^{9,10} and use of only a short spacer¹¹ favor formation of a nematic mesophase. In addition, the 1,4-bis(benzoyloxy)benzene mesogens tend to form only nematic mesophases, especially at these *n*-alkoxy substituent lengths.¹ Therefore, we expect that some combinations of hydrocarbon and fluorocarbon lengths will

* To whom correspondence should be addressed.

Scheme 2. Synthesis of the 2,5-Bis[(4'-*n*-(perfluoroalkyl)alkoxy)benzoyl]oxy]toluene Model Compounds with *m* = 3–4 (*n* = 3–6,8)



Scheme 3. Synthesis of the 2,5-Bis[(4'-*n*-(perfluoroalkyl)alkoxy)benzoyl]oxy]toluene Model Compounds with *m* = 2 (*n* = 3–6,8)



be effective at inducing smectic layering in the low molar mass model compounds, but not in the corresponding SCLCPs.

Results and Discussion

Synthesis and Thermotropic Behavior of the Model Compounds. The 2,5-bis{[4'-(*n*-(perfluoroalkyl)alkoxy)benzoyl]oxy}toluene model compounds were prepared by the routes shown in Schemes 2 and 3. Due to the insolubility of 4-[*n*-(perfluoroalkyl)alkoxy]benzoic acids with longer hydrocarbon and fluorocarbon segments, we previously synthesized the model compounds with *n* = 4–6,8 and *m* = 6–8 by constructing the mesogen first and then introducing the fluorocarbon segments.⁴ As shown in Scheme 2, we also prepared the model compounds with *n* = 3–6,8 and *m* = 3–4 by this route. Ethyl 4-(ω -bromo-1-alkenyloxy)benzoate was etherified with an ω -bromo-1-alkene, followed by saponification of the ester group under basic conditions to produce the 4-*n*-(alkenyloxy)benzoic acids. The mesogenic core was then generated by coupling the 4-*n*-(alkenyloxy)benzoic acids with methylhydroquinone in the presence of dicyclohexylcarbodiimide (DCC) as a dehydrating agent. The perfluoroalkyl groups were introduced by free radical

Table 1. Thermal Transitions and Thermodynamic Parameters of 2,5-Bis[(4'-*n*-(perfluoroalkyl)alkoxy)benzoyl]oxy]toluenes^a

<i>n</i>	<i>m</i>	phase transitions, °C (ΔH , kJ/mol)				
3	2	k 112 (47.1)		<i>s_A</i> 145 (0.357)	<i>n</i> 155 (1.06)	i
4	2	k 109 (50.8)		<i>s_A</i> 113 (0.377)	<i>n</i> 154 (1.54)	i
5	2	k 96 (41.1)	<i>s_C</i> 82 ^b	<i>s_A</i> 151 ^b	<i>n</i> 151 (4.14)	i
6	2	k 97 (44.4)	<i>s_C</i> 117 ^b	<i>s_A</i> 151 (1.90)	<i>n</i> 152 (2.94)	i
8	2	k 103 (70.6)	<i>s_C</i> 104 ^b	<i>s_A</i> 149 (6.97)		i
3	3	k 122 (26.3)	<i>s_C</i> 119 ^b	<i>s_A</i> 184 (4.41)		i
4	3	k 105 (38.6)	<i>s_C</i> 152 (0.078)	<i>s_A</i> 169 (5.80)		i
5	3	k 88 (24.7)	<i>s_C</i> 123 ^b	<i>s_A</i> 174 (7.25)		i
6	3	k 99 (59.1)	<i>s_C</i> 147 ^b	<i>s_A</i> 169 (8.22)		i
8	3	k 105 (60.6)	<i>s_C</i> 149 ^b	<i>s_A</i> 162 (10.1)		i
3	4	k 110 (26.7)	<i>s_C</i> 157 (0.083)	<i>s_A</i> 199 (5.97)		i
4	4	k 96 (26.7)	<i>s_C</i> 173 (0.135)	<i>s_A</i> 189 (7.58)		i
5	4	k 86 (22.5)	<i>s_C</i> 162 (0.086)	<i>s_A</i> 186 (7.76)		i
6	4	k 113 (45.3)	<i>s_C</i> 172 (0.084)	<i>s_A</i> 185 (7.18)		i
8	4	k 94 (57.4)	<i>s_C</i> 169 (0.150)	<i>s_A</i> 176 (9.76)		i

^a Observed on heating; k = crystalline, *s_C* = smectic C, *s_A* = smectic A, *n* = nematic, and i = isotropic; *n* methylenic units, *m* perfluoromethylene units. ^b Transition detected only by polarized optical microscopy.

addition of a perfluoroalkyl iodide across the double bonds of the *n*-alkenyloxy substituents, followed by reduction of the resulting alkyl iodide using tributyltin hydride under free radical conditions. The model compounds with the shortest fluorocarbon length (*m* = 2) were readily synthesized by functionalizing the substituents first, and then constructing the mesogen (Scheme 3). Although the order is different, all of the steps in Scheme 3 are analogous to those in Scheme 2.

Table 1 summarizes the thermal transitions of the 15 model compounds. The data were obtained on heating and are from thermally equilibrated samples, i.e., samples that were recrystallized from solution and/or from the melt after short annealing times. In most cases, crystallization from the melt to the most thermodynamically stable phase is slower than the time scale of the differential scanning calorimetry (DSC) experiment. This results in either incomplete recrystallization or crystallization to a less stable crystalline phase if sufficient annealing time is not allowed.

We identified the mesophases by polarized optical microscopy. In contrast to the model compounds with longer hydrocarbon and fluorocarbon segments,⁴ these compounds do not tend to align homeotropically, and it therefore was not necessary to pretreat the glass slides with a hydrocarbon solvent. Figure 1a shows a representative schlieren nematic texture,¹² with both two-brush and four-brush singularities, that was observed upon cooling the *n*, *m* = 6, 2 model compound from the isotropic melt. Further cooling into the smectic A (*s_A*) phase yielded a typical focal-conic fan texture¹² (Figure 1b) and into the smectic C (*s_C*) phase yielded a typical paramorphotic broken focal-conic fan texture¹² (Figure 1c).

Figures 2 and 3 plot the isotropization temperature of the model compounds as a function of the total number of carbons in both the hydrocarbon and fluorocarbon segments (*n* + *m*) and the number of carbons (*n*) in the hydrocarbon segments, respectively, including those prepared previously⁴ with longer hydrocarbon and fluorocarbon segments. Both figures also plot the temperature of the nematic–isotropic transitions of their hydrocarbon analogues,^{10,13,14} (*m* = 0). In general, all of the transition temperatures decrease with increasing hydrocarbon length as the molecules become more like

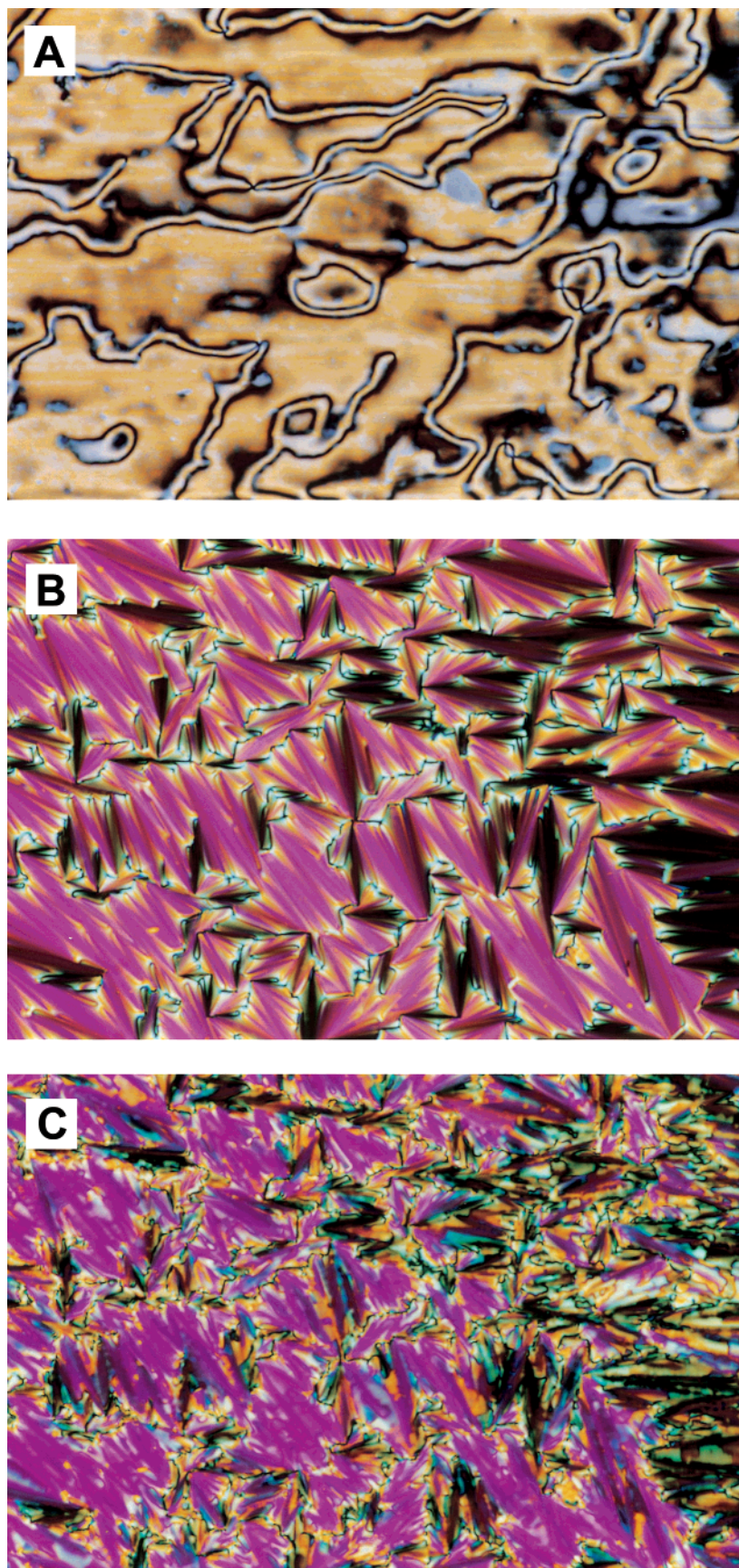


Figure 1. Polarized optical micrographs (200 \times) observed on cooling 2,5-bis[(4'-*n*-((perfluoroethyl)hexoxy)benzoyl)oxy]toluene (n , $m = 6, 2$) from the isotropic melt: (a) 151 $^{\circ}\text{C}$, nematic schlieren texture; (b) 130 $^{\circ}\text{C}$, s_A focal-conic fan texture; (c) 101 $^{\circ}\text{C}$, s_C paramorphotic broken focal-conic fan texture.

polyethylene (HDPE $T_m = 138\text{ }^{\circ}\text{C}^{15}$), and increase with increasing fluorocarbon length as they become more like

poly(tetrafluoroethylene) (PTFE $T_m = 332\text{ }^{\circ}\text{C}^{15}$). As shown in Figure 2, when the isotropization temperature

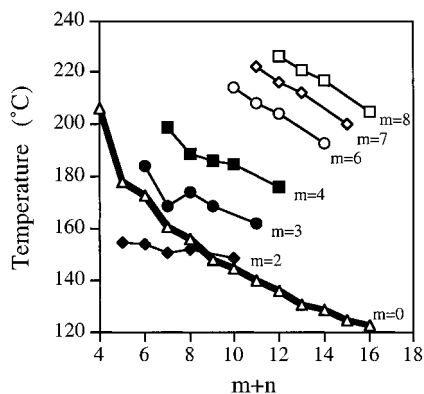


Figure 2. Temperature of isotropization of 2,5-bis[(4'-*n*-(perfluoroalkyl)alkoxy)benzoyl]oxy]toluenes as a function of the total number of carbons in the *n*-alkoxy substituents at various fluorocarbon lengths (*m* perfluoromethylene units).

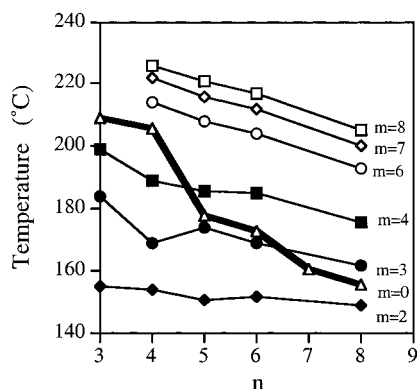


Figure 3. Temperature of isotropization of 2,5-bis[(4'-*n*-(perfluoroalkyl)alkoxy)benzoyl]oxy]toluenes as a function of the number of carbons (*n*) in the hydrocarbon substituents at various fluorocarbon lengths (*m* perfluoromethylene units).

is plotted as a function of the total number of methylenic units in the *n*-(perfluoroalkyl)alkoxy substituents, the temperatures of isotropization of the fluorinated model compounds are generally higher than those of the hydrocarbon analogues. The only exceptions are the *m* = 2 compounds that, like the hydrocarbon analogues, undergo isotropization from a nematic mesophase rather than from a *s_A* mesophase. The point at which the clearing temperature changes from a nematic–isotropic (i) to a *s_A*–i transition is the point at which the *T_i* vs *m* + *n* line crosses the *m* = 0 line on the graph.

As summarized in Table 1, terminating the *n*-alkoxy substituents of the nematic model compounds with fluorocarbon segments of three or four perfluoromethylene units is still effective at inducing smectic layering; all of the fluorinated model compounds with *m* = 3–4 exhibit a crystalline (k)–*s_C*–*s_A*–i phase sequence. In contrast, the *m* = 2 model compounds exhibit a nematic phase in addition to the *s_A* phase when *n* = 3–4; the *m* = 2 model compounds with *n* = 5–6 exhibit a nematic phase in addition to both *s_A* and *s_C* mesophases. Only the *m* = 2 model compound with the longest hydrocarbon segment (*n*, *m* = 8, 2) exhibits only smectic mesophases. This indicates that the hydrocarbon and fluorocarbon segments are not microphase separated when *m* = 2 and *n* = 3–6 and that their smectic mesophases are not the result of immiscibility between the two segments.

As discussed previously for the model compounds whose hydrocarbon (*n* ≥ 4) and fluorocarbon (*m* ≥ 6)

Table 2. Changes in Enthalpy per Methylenic Unit for the Thermal Transitions of the 2,5-Bis[(4'-*n*-(perfluoroalkyl)alkoxy)benzoyl]oxy]toluenes with Longer Hydrocarbon and Fluorocarbon Segments^a

<i>n</i>	<i>m</i>	change in enthalpy (kJ/mol)		
		$\Delta H_m/n$	$\Delta H_{s_C-s_A}/m$	$\Delta H_i/(n+m)$
4	6	11	0.077	0.88
5	6	4.8	0.072	0.99
6	6	8.2	0.077	0.87
8	6	6.3	0.10	0.71
4	7	11	0.099	0.61
5	7	7.1	0.13	0.70
6	7	7.6	0.090	0.52
8	7	6.4	0.11	0.51
4	8	12	0.14	0.72
5	8	6.5	0.16	0.62
6	8	9.8	0.18	0.63
8	8	6.9	0.20	0.58
mean		8.1 ± 2.2	0.12 ± 0.041	0.70 ± 0.14

^a Calculated from the data observed on heating in ref 4; *n* methylenic units, *m* perfluoromethylene units.

segments are presumably long enough to microphase separate,⁴ the hydrocarbon and fluorocarbon segments apparently disorder separately at different transitions. On the basis of the relatively constant, albeit with a slight odd–even alternation, change in enthalpy at the k–*s_C* transition for a given hydrocarbon length as a function of fluorocarbon length, the linear hydrocarbon segments apparently disorder primarily at the crystalline melting transition. Therefore, as summarized in Table 2, the change in enthalpy per methylenic unit at melting ($\Delta H_m/n$) is relatively constant at 8.1 ± 2.2 kJ/mol. Based on the invariant change in enthalpy at the *s_C*–*s_A* transition to changes in the hydrocarbon length for a given fluorocarbon, the fluorocarbon segments apparently disorder primarily at the *s_C*–*s_A* transition. Therefore, the change in enthalpy at the *s_C*–*s_A* transition per perfluoromethylene unit ($\Delta H_{s_C-s_A}/m$) is relatively constant at 0.12 ± 0.041 kJ/mol (Table 2). The change in enthalpy of isotropization is independent of both hydrocarbon and fluorocarbon length, which indicates that the molecules finally lose their orientational order at isotropization, and the change in enthalpy of isotropization per total number of methylenic and perfluoromethylene groups [$\Delta H_i/(n+m)$] is essentially constant at 0.70 ± 0.14 kJ/mol (Table 2).

These values may be useful for elucidating which hydrocarbon and fluorocarbon lengths of the new model compounds with shorter fluorocarbon segments are microphase separated; Table 1 lists the enthalpy changes associated with their transitions. As shown in Table 3, the values of $\Delta H_m/n$ and $\Delta H_i/(n+m)$ deviate significantly from the values in Table 2 only for the two compounds with the shortest hydrocarbon and fluorocarbon segments (*n* = 3, 4, *m* = 2). This indicates that the hydrocarbon and fluorocarbon segments of only these two compounds are not microphase separated. However, the two *m* = 2 compounds with *n* = 5, 6 also exhibit a nematic mesophase, in which the two segments must be mixed, before undergoing isotropization. In addition, all of the $\Delta H_m/m$ values in Table 3 are significantly lower than those in Table 2, which might indicate that the hydrocarbon and fluorocarbon segments are not microphase separated in any of the model compounds with shorter fluorocarbon segments (*m* = 2–4).

The plots in Figure 3 may help resolve this discrepancy. If the hydrocarbon and fluorocarbon segments are

Table 3. Changes in Enthalpy per Methylenic Unit for the Thermal Transitions of the 2,5-Bis[(4'-*n*-(perfluoroalkyl)alkoxy)benzoyl]oxy]toluenes with Short Fluorocarbon Segments^a

<i>n</i>	<i>m</i>	change in enthalpy (kJ/mol)		
		$\Delta H_m/n$	$\Delta H_{s_C-s_A}/m$	$\Delta H/n+m^2$
3	2	16		0.28
4	2	13		0.32
5	2	8.2	<i>b</i>	0.59
6	2	7.4	<i>b</i>	0.60
8	2	8.8	<i>b</i>	0.70
3	3	8.8	<i>b</i>	0.74
4	3	9.6	0.026	0.83
5	3	4.9	<i>b</i>	0.91
6	3	9.8	<i>b</i>	0.91
8	3	7.6	<i>b</i>	0.92
3	4	8.9	0.021	0.85
4	4	6.7	0.034	0.95
5	4	4.5	0.022	0.86
6	4	7.6	0.021	0.72
8	4	7.2	0.038	0.82

^a Change in enthalpy of the s_A-i transition (all $m = 3$; all $m = 4$; $n, m = 8, 2$) or the sum of the s_A-n-i transitions (all $m=2$ except $n=8$); n methylenic units, m perfluoromethylenic units. ^b Transition detected only by polarized optical microscopy.

microphase separated, then the chemical structure of the immiscible segment should have little influence on the transition temperatures relative to the hydrocarbon analogues with the same number of methylenic units in their *n*-alkoxy substituents, except as a weighting factor at the hydrocarbon-fluorocarbon interface, which restricts the motions of the hydrocarbon segments and thereby increases the transition temperatures. Therefore, we suspect that the hydrocarbon and fluorocarbon segments are not inherently microphase separated in any of the 11 compounds in Figure 3 whose isotropization temperatures are lower than those of the hydrocarbon analogues. This includes all of the $m = 2$ compounds, the $m = 3$ compounds with the four shortest hydrocarbon segments ($n = 3-6$), and the $m = 4$ compounds with the two shortest hydrocarbon segments ($n = 3, 4$). In these cases, the smectic mesophases may arise because of the high polarity of the molecules due to the fluorocarbon segments. The remaining four compounds with longer hydrocarbon segments in the $m = 3$ and $m = 4$ series have higher isotropization temperatures than their hydrocarbon analogues, which indicates that their hydrocarbon and fluorocarbon segments are microphase separated.

Synthesis and Thermotropic Behavior of the Monomers. As outlined in Scheme 4, the monomers were synthesized directly from the model compounds by free radical bromination at the benzylic position, followed by phase transfer catalyzed esterification with potassium bicyclo[2.2.1]hept-2-ene-5-carboxylate.

Table 4 summarizes the thermotropic behavior of the equilibrated monomers. The monomers prepared previously with $m = 6-8$ generally exhibited an enantiotropic s_A mesophase and a monotropic s_C mesophase,⁴ which was observed only on cooling; the isotropization and crystalline melting transition temperatures were also lower than those of the model compounds. That is, lateral substitution of the model compounds at the benzylic position with a bulky norbornyl group suppresses all of the transition temperatures, especially that of the s_C-s_A transition, due to the decreased packing density. The additional bulk of the norbornyl group has an even greater effect on the new monomers

Scheme 4. Synthesis of the 5-[[[2',5'-Bis[(4'-*n*-(perfluoroalkyl)alkoxy)benzoyl]oxy]benzyl]oxy]carbonyl]bicyclo[2.2.1]hept-2-ene Monomers

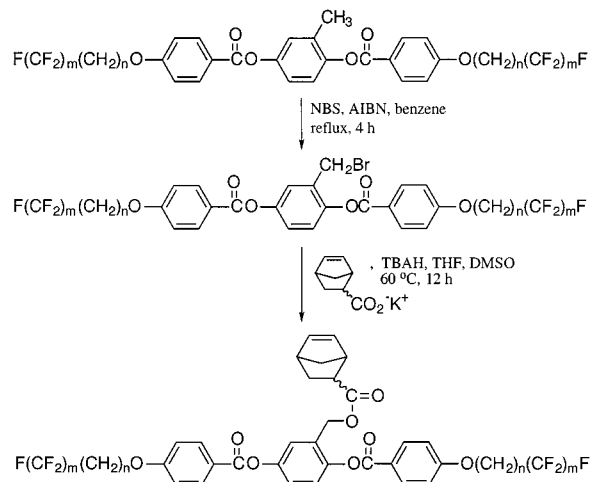


Table 4. Thermal Transitions and Thermodynamic Parameters of 5-[[[2',5'-Bis[(4'-*n*-(perfluoroalkyl)alkoxy)benzoyl]oxy]benzyl]oxy]carbonyl]bicyclo[2.2.1]hept-2-enes^a

<i>n</i>	<i>m</i>	% endo	phase transitions, °C (ΔH , kJ/mol)			
3	2	67	k 111 (54.6)			i
4	2	75	k 112 (38.2)			i
5	2	62	k 79 (29.6)			i
6	2	67	k 91 (60.1)		[n 47] ^b	i
8	2	67	k 54 (23.1)		n 57 (1.73)	i
3	3	59	k 97 (25.0)			i
4	3	31	k 101 (29.0)			i
5	3	57	k 76 (22.5)	s_A 82 (3.19)		i
6	3	75	k 65 (19.9)	s_A 80 (3.19)		i
8	3	25	k 56 (23.3)	[s_C 31] ^b s_A 82 (4.50)		i
3	4	65	k 53 (16.7)	[s_C 44] ^b s_A 115 (3.49)		i
4	4	67	k 88 (23.8)	[s_C 74] ^b s_A 107 (3.74)		i
5	4	73	k 83 (32.5)	s_A 114 (4.41)		i
6	4	45	k 68 (20.6)	[s_C 51] ^b s_A 114 (5.00)		i
8	4	31	k 58 (32.5)	s_A 108 (5.52)		i

^a Observed on heating; k = crystalline, s_C = smectic C, s_A = smectic A, n = nematic, and i = isotropic; [monotropic]; n methylenic units, m perfluoromethylenic units. ^b Transition detected only by polarized optical microscopy.

with shorter fluorocarbon segments. In this case, the monomers with both short hydrocarbon ($n = 3-4$ or 5) and short fluorocarbon ($m = 2-3$) segments do not exhibit any liquid crystalline phases, and the $n, m = 6, 2$ monomer exhibits only a monotropic nematic mesophase. In addition, the smectic mesophases of the $n, m = 8, 2$ model compound have been converted to a nematic mesophase in the corresponding monomer. As summarized in Table 4, the enthalpy changes associated with these transitions are also smaller than those of the model compounds.

Synthesis and Thermotropic Behavior of the Polymers. The poly{5-[[[2',5'-bis[(4'-*n*-(perfluoroalkyl)alkoxy)benzoyl]oxy]benzyl]oxy]carbonyl]bicyclo[2.2.1]hept-2-ene}s were prepared by ring-opening metathesis polymerization (ROMP) of the monomers as shown in Scheme 5. The polymerizations were carried out at 25 °C in a drybox using extensively degassed THF as the solvent and Mo(N-2,6-*i*-Pr₂Ph)(CHCMe₂Ph)(O-*t*-Bu)₂ as the initiator, then quenched after 2 h with benzaldehyde. Unlike the polymers with $m = 6-8$,⁴ the poly-norbornenes with $m = 2-4$ were completely soluble in THF at room temperature, and the solutions remained

Scheme 5. Ring-Opening Metathesis Polymerization of 5-[[[2',5'-Bis(4''-*n*-(perfluoroalkyl)alkoxy)benzoyl]oxy]benzyl]oxy]carbonyl]bicyclo[2.2.1]hept-2-enes

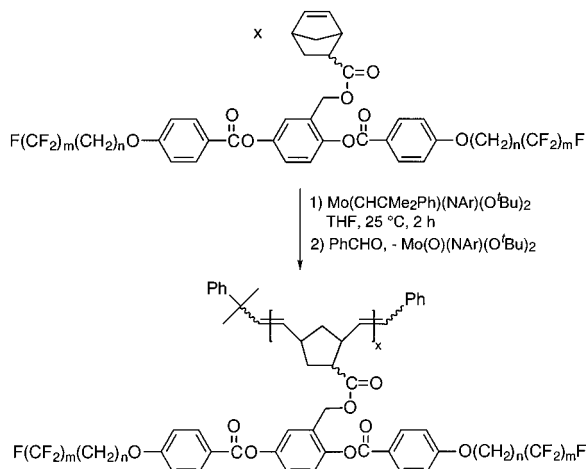


Table 5. Polymerization of 5-[[[2',5'-Bis(4''-*n*-(perfluoroalkyl)alkoxy)benzoyl]oxy]benzyl]oxy]carbonyl]bicyclo[2.2.1]hept-2-enes and Characterization of the Resulting Polymers^a

<i>n</i>	<i>m</i>	[M] ₀ /[I] ₀	yield (%)	GPC ^b		
				<i>M_n</i> × 10 ⁻⁴	DP _n	pdi
3	2	50	88	3.24	40	1.43
4	2	54	39	7.59	89	1.47
5	2	50	34	3.12	36	1.34
6	2	52	82	2.26	25	1.40
8	2	45	18	3.03	31	1.49
3	3	49	84	9.98	108	1.36
4	3	52	20	1.38	15	1.16
5	3	38	86	4.37	45	1.28
6	3	49	82	4.36	43	1.32
8	3	51	92	2.75	26	1.25
3	4	52	75	4.61	45	1.34
4	4	50	78	6.06	58	1.45
5	4	50	75	7.44	69	1.57
6	4	53	65	4.37	40	1.45
8	4	50	80	5.99	52	1.39

^a Polymerized in THF at room temperature for 2 h; *n* methylenic units, *m* perfluoromethylenic units. ^b Number average molecular weight (*M_n*), number average degree of polymerization (DP_n), and polydispersity (pdi = *M_w*/*M_n*) determined by gel permeation chromatography (GPC) relative to polystyrene.

homogeneous throughout the polymerization. In almost all cases, however, the polymers were contaminated with a low molecular weight tail, and in some cases a double molecular weight shoulder due to oxygen.¹⁶ Hence the polymers were purified by fractional precipitation prior to thermal analysis. Table 5 summarizes the final molecular weights and molecular weight distributions (pdi) of the polymers used for thermal analysis. The polynorbornenes generally had a degree of polymerization (DP_n) greater than 25, which is the minimum required for the thermotropic behavior of mesogenic polynorbornenes to be independent of molecular weight.^{10,11}

Table 6 summarizes the thermal transitions of the 15 polynorbornenes. The data were obtained on heating and are from thermally equilibrated samples. In contrast to the model compounds, terminating the *n*-alkoxy substituents of the nematic polymers with fluorocarbon segments of three or four perfluoromethylenic units is only effective at inducing smectic layering when the hydrocarbon segment contains at least eight or five methylenic units, respectively; these compounds exhibit

Table 6. Thermal Transitions and Thermodynamic Parameters of Poly{5-[[[2',5'-bis(4''-*n*-(perfluoroalkyl)alkoxy)benzoyl]oxy]benzyl]oxy]carbonyl]bicyclo[2.2.1]hept-2-ene}s^a

<i>n</i>	<i>m</i>	phase transitions, °C (Δ <i>H</i> , kJ/mru)		
		g	s _A	i
3	2	g 76		i
4	2	g 75	n 99 (2.00)	i
5	2	g 65	n 94 (0.777)	i
6	2	g 65	n 102 (1.30)	i
8	2	g 61	n 104 (1.21)	i
3	3	g 81	n 106 (0.855)	i
4	3	g 85	n 108 (0.834)	i
5	3	g 75	n 120 (0.798)	i
6	3	g 90	n 124 (1.18)	i
8	3	g 61	s _A 139 (3.18)	i
3	4	g 96	n 137 (0.710)	i
4	4	g 91	n 144 (1.18)	i
5	4	g 81	s _A 164 (2.59)	i
6	4	g 77	s _A 171 (3.06)	i
8	4	g 81	s _A 169 (4.00)	i

^a Observed on heating; g = glass, s_C = smectic C, s_A = smectic A, and i = isotropic; *n* methylenic units, *m* perfluoromethylenic units; mru = moles repeat unit.

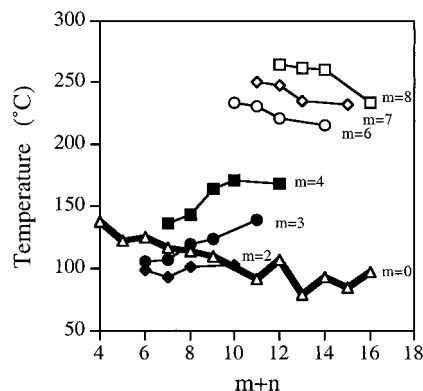


Figure 4. Temperature of isotropization of poly{5-[[[2',5'-bis(4''-*n*-(perfluoroalkyl)alkoxy)benzoyl]oxy]benzyl]oxy]carbonyl]bicyclo[2.2.1]hept-2-ene}s as a function of the total number of carbons in the *n*-alkoxy substituents at various fluorocarbon lengths (*m* perfluoromethylenic units).

a s_A mesophase. The *m* = 3 and *m* = 4 polymers with shorter hydrocarbon segments, and with the exception of the *n*, *m* = 3, 2 polymer, all of the *m* = 2 polymers exhibit only a nematic mesophase. The changes in the enthalpy of isotropization reported in Table 6 are also consistent with those of the n-i and s_A-i transitions reported previously⁴ for the polymers with longer hydrocarbon and fluorocarbon segments, and in Table 1 for the model compounds.

A polarized optical micrograph is presented in the Supporting Information which is representative of the texture observed for the majority of the SCLCPs presented in Table 6. The nematic schlieren texture grows in via tiny droplets, and although highly threaded, the 2- and 4-brush singularities are visible. The polymers with a s_A mesophase first exhibit well-defined batonnets on cooling from the isotropic melt before developing into an ill-defined, highly threaded texture.

Figures 4 and 5 plot the isotropization temperature of the polymers as a function of the total number of carbons in both the hydrocarbon and fluorocarbon segments (*n* + *m*) and the number of carbons (*n*) in the hydrocarbon segments, respectively, for fluorocarbon lengths of *m* = 2–4 and *m* = 6–8.⁴ Both figures also plot the temperature of the nematic–isotropic transitions of their hydrocarbon analogues^{10,13} (*m* = 0). All of

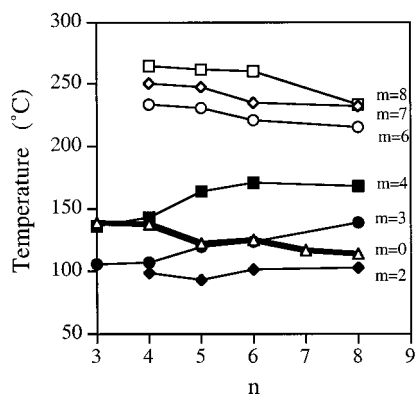


Figure 5. Temperature of isotropization of poly{5-[[[2',5'-bis-(4'-*n*-(perfluoroalkyl)alkoxy)benzoyl]oxy]benzyl]oxy]carbonyl-bicyclo[2.2.1]hept-2-ene}s as a function of the number of carbons (*n*) in the hydrocarbon substituents at various fluorocarbon lengths (*m* perfluoromethylene units).

the polymers whose isotropization temperatures are at or below the T_i vs *n* line in Figure 5 for the hydrocarbon analogues (*m* = 0) undergo isotropization from a nematic mesophase rather than from a S_A mesophase. However, a few of the polymers with nematic mesophases have isotropization temperatures slightly above the T_i vs *n* + *m* line in Figure 4 for the hydrocarbon analogues (*m* = 0). In addition, unlike the SCLCPs with *m* = 6–8 and all of the model compounds, the transition temperatures increase with increasing hydrocarbon length. This suggests that the hydrocarbon and fluorocarbon segments of the polymers are not microphase separated when *m* ≤ 4.

Conclusions

Nematic LMMLCs and laterally attached side-chain liquid crystalline polynorbornenes with 1,4-bis[(4'-*n*-alkoxybenzoyl)oxy]benzene mesogens can be forced to order into smectic layers by terminating their *n*-alkoxy substituents with fluorocarbon segments. Since aliphatic hydrocarbons and fluorocarbons are highly immiscible,¹⁷ we attribute this layered organization to microphase separation of the two components of the amphiphilic substituents; however, the immiscibility of *n*-alkanes and *n*-perfluoroalkanes is directly proportional to their lengths.¹⁸ In contrast to this concept for inducing smectic layering in nematic liquid crystals, smectic liquid crystals can be converted to nematic liquid crystals by laterally substituting the mesogen with bulky groups.³ Therefore, as the bulk of the lateral substituent on the 1,4-bis{[4'-(*n*-(perfluoroalkyl)alkoxy)benzoyl]oxy}benzene mesogens increases from methyl, to norbornyl, to polynorbornyl, increasingly longer hydrocarbon and/or fluorocarbon segments are required to induce smectic layering. The 2,5-bis{[4'-(*n*-(perfluoroalkyl)alkoxy)benzoyl]oxy}toluene model compounds exhibit only smectic mesophases when the hydrocarbon and fluorocarbon segments are both as short as three methylenic units. The norbornene monomers exhibit smectic mesophases when the hydrocarbon and fluorocarbon segments are as short as five and three, or three and four, methylenic units, respectively. The polynorbornenes require at least eight and three, or five and four, methylenic units in the hydrocarbon and fluorocarbon segments, respectively, to organize into smectic layers. Nevertheless, on the basis of the isotropization temperatures relative to their hydrocarbon analogues

and changes in enthalpy at each transition, microsegregation of the two components in these amphiphilic molecules is apparently weak at the minimum lengths required for smectic layering.

Experimental Section

Materials. Acryloyl chloride (96%), 4-bromo-1-butene (97%), 8-bromo-1-octene (98%), 5-bromo-1-pentene (97%), ethyl 4-hydroxybenzoate (99%), methyl hydroquinone (99%), pentafluoroethyl iodide (97%), perfluorobutyl iodide (98%), and tetrabutylammonium hydrogen sulfate (TBAH, 99%) were used as received from Aldrich. Allyl bromide (Lancaster), 6-bromo-1-hexene (Fluka, 95%), 1,3-dicyclohexylcarbodiimide (DCC, 99%, Acros), 4-(dimethylamino)pyridine (DMAP, Lancaster, 99%), heptafluoropropyl iodide (Lancaster, 98%), *p*-toluenesulfonic acid (Mallinckrodt), and tributyltin hydride (Fluka, 97%) were also used as received. 2,2'-Azobisisobutyronitrile (AIBN, Kodak) was recrystallized from methanol below 40 °C. Benzaldehyde (Aldrich, 99%) was distilled under N_2 before use. *N*-Bromosuccinimide (NBS, Aldrich, 99%) was recrystallized from boiling water. Cyclopentadiene was freshly cracked from dicyclopentadiene (Aldrich, 95%). Mo(CHCMe₂-Ph)(N-2,6-*Pr*₂Ph)(O^tBu)₂ was synthesized by a literature procedure,¹⁹ except that hexanes were used throughout the synthesis instead of pentane, or purchased from Strem and used after recrystallization from dry hexanes. Potassium bicyclo[2.2.1]hept-2-ene-5-carboxylate (68% endo, 32% exo) was synthesized as previously reported.⁴ CH_2Cl_2 was washed with 10% HNO_3 in H_2SO_4 , stored over $CaCl_2$, and then distilled from CaH_2 under N_2 . Reagent grade dimethyl sulfoxide (DMSO) was dried by distillation from CaH_2 under N_2 . Hexanes used in all drybox procedures were washed with 5% HNO_3 in H_2SO_4 , stored over $CaCl_2$, and then distilled from purple sodium benzophenone ketyl under N_2 . Reagent grade tetrahydrofuran (THF) and toluene were dried by distillation from purple sodium benzophenone ketyl under N_2 . THF used as a polymerization solvent was vacuum transferred from purple sodium benzophenone ketyl on a high vacuum line and then vigorously degassed by several freeze–pump–thaw cycles immediately before use. All other reagents and solvents were commercially available and used as received.

Techniques. All polymerizations were performed under a N_2 atmosphere in a Vacuum Atmospheres drybox. All other reactions were performed outside the drybox under a N_2 atmosphere. ¹H NMR spectra (δ , ppm) were recorded on a Bruker AC-200 (200 MHz), Bruker AM-300 (300 MHz), Mercury 300 (300 MHz), Bruker AM-360 (360 MHz), or a Varian Unity INOVA 400 (400 MHz) spectrometer. Unless noted otherwise, all spectra were recorded in $CDCl_3$. ¹H resonances were measured relative to residual solvent resonances and referenced to Me_4Si . Relative molecular weights were determined by gel permeation chromatography (GPC) at 35 °C using THF as solvent (1.0 mL/min), a set of 50, 100, 500, 10⁴, and linear (50–10⁴) Å Styragel 5 μ columns, a Waters 486 tunable UV/Vis detector set at 290 nm, and a Waters 410 differential refractometer. Elemental analyses were performed on a PE 2400 Series II CHNS/O Analyzer by CHN/AA services, Department of Chemistry, University of Michigan. Two analyses were performed on each sample submitted, and the average values are reported.

The thermotropic behavior of all compounds was determined by a combination of differential scanning calorimetry (DSC) and polarized optical microscopy. A Perkin-Elmer DSC-7 differential scanning calorimeter was used to determine the thermal transitions, which were read as the maximum or minimum of the endothermic or exothermic peaks, respectively. Glass transition temperatures (T_g s) were read as the middle of the change in heat capacity. All heating and cooling rates were 10 °C/min. Both enthalpy changes and transition temperatures were determined using indium as a calibration standard. All samples were initially heated three times and cooled twice; their equilibrium transition temperatures and enthalpies were subsequently determined through extensive annealing and quenching studies. A Leitz Laborlux 12 Pol S

polarized optical microscope (magnification 200x) equipped with a Mettler FP82 hot stage and a Mettler FP90 central processor was used to observe the thermal transitions and to analyze the anisotropic textures.¹² Thin samples were prepared by melting a minimum amount of compound between a clean glass slide and a cover slip and rubbing the cover slip with a spatula.

Synthesis of Monomers and Precursors. Ethyl 4-(*n*-Alkenyloxy)benzoates (*n* = 3–6, 8). Ethyl 4-(*n*-prop-2'-enyloxy)benzoate was prepared in 81% yield as described previously for the ethyl 4-(*n*-alkenyloxy)benzoates⁴ with *n* = 4–6, 8. ¹H NMR: 1.37 (t, *J* = 7.1 Hz, CH₃CH₂O₂C), 4.34 (q, *J* = 7.1 Hz, CH₂O₂C), 4.59 (dt, *J* = 5.3, 1.5 Hz, OCH₂), 5.31 (dq, *J* = 10.5, 1.4 Hz, *E*-HCH=CH), 5.42 (dq, *J* = 17.3, 1.6 Hz, *Z*-HCH=CH), 6.05 (ddt, *J* = 17.3, 10.4, 5.3 Hz, CH=CH₂), 6.92 (AA'XX', 2 aromatic H *ortho* to OCH₂), 7.99 (AA'XX', 2 aromatic H *ortho* to CO₂).

Ethyl 4-(*n*-Pentafluoroethyl)alkoxy)benzoates (*n* = 3–6, 8; *m* = 2). The ethyl 4-(*n*-pentafluoroethyl)alkoxy)benzoates were synthesized in 36–68% yield as in the following example. Ethyl 4-(*n*-prop-2'-enyloxy)benzoate (4.1 g, 20 mmol) and AIBN (0.32 g, 2.0 mmol) were placed in a 100 mL heavy walled glass reactor. The reactor was placed in liquid N₂ for 20 min, a slight vacuum was pulled, and then pentafluoroethyl iodide (8.5 g, 35 mmol) was condensed into the flask. The solution was degassed by several freeze–pump–thaw cycles and then heated at 70 °C under a static vacuum. After 16 h, the conversion was determined by ¹H NMR and the above process was repeated until over 95% of the ethyl 4-(*n*-prop-2'-enyloxy)benzoate was consumed. AIBN (0.50 g, 3.0 mmol) and tributyltin hydride (8.0 mL, 30 mmol) were then added to the reactor and the reaction heated at 70 °C under N₂ for 2 h. After ¹H NMR demonstrated that the reduction was complete, the mixture was dissolved in CH₂Cl₂/hexanes/petroleum ether (5:2:1, 20 mL) and purified by repeated column chromatography using silica gel as the stationary phase and CH₂Cl₂/hexanes/petroleum ether (5:2:1) as the eluent. The solvent was removed in vacuo to yield 2.9 g (44%) of ethyl 4-(*n*-pentafluoroethyl)propoxy)benzoate as a white solid. Recrystallization from dry hexanes (30 mL) yielded 2.3 g (36%) of a white crystalline solid, mp = 73 °C. ¹H NMR: 1.38 (t, *J* = 7.1 Hz, CH₃CH₂O₂C), 2.12 (m, CH₂CH₂CF₂), 2.26 (m, CH₂CF₂), 4.09 (t, *J* = 5.9 Hz, OCH₂), 4.35 (q, *J* = 7.1 Hz, CH₂O₂C), 6.90 (AA'XX', 2 aromatic H *ortho* to OCH₂), 8.00 (AA'XX', 2 aromatic H *ortho* to CO₂). Anal. Calcd for C₁₄H₁₅F₅O₃: C, 51.54; H, 4.63. Found: C, 51.55; H, 4.57.

Ethyl 4-(*n*-Pentafluoroethyl)butoxy)benzoate. Mp = 44 °C. ¹H NMR: 1.38 (t, *J* = 7.1 Hz, CH₃CH₂O₂C), 1.81 (m, CH₂CH₂CF₂), 1.87 (m, CH₂CH₂O), 2.12 (m, CH₂CF₂), 4.05 (t, *J* = 5.9 Hz, OCH₂), 4.35 (q, *J* = 7.1 Hz, CH₂O₂C), 6.90 (AA'XX', 2 aromatic H *ortho* to OCH₂), 7.99 (AA'XX', 2 aromatic H *ortho* to CO₂). Anal. Calcd for C₁₅H₁₇F₅O₃: C, 52.94; H, 5.04. Found: C, 52.73; H, 4.83.

Ethyl 4-(*n*-Pentafluoroethyl)pentoxy)benzoate. Mp = 60 °C. ¹H NMR: 1.38 (t, *J* = 7.1 Hz, CH₃CH₂O₂C), 1.58 (m, CH₂CH₂CH₂CF₂), 1.68 (m, CH₂CH₂CF₂), 1.85 (m, CH₂CH₂O), 2.06 (m, CH₂CF₂), 4.02 (t, *J* = 6.2 Hz, OCH₂), 4.34 (q, *J* = 7.1 Hz, CH₂O₂C), 6.89 (AA'XX', 2 aromatic H *ortho* to OCH₂), 7.99 (AA'XX', 2 aromatic H *ortho* to CO₂). Anal. Calcd for C₁₆H₁₉F₅O₃: C, 54.24; H, 5.40. Found: C, 53.98; H, 5.45.

Ethyl 4-(*n*-Pentafluoroethyl)hexoxy)benzoate. Mp = 42 °C. ¹H NMR: 1.38 (t, *J* = 7.1 Hz, CH₃CH₂O₂C), 1.50 (m, (CH₂)₂CH₂CH₂CF₂), 1.63 (m, CH₂CH₂CF₂), 1.82 (m, CH₂CH₂O), 2.03 (m, CH₂CF₂), 4.01 (t, *J* = 6.3 Hz, OCH₂), 4.34 (q, *J* = 7.1 Hz, CH₂O₂C), 6.89 (AA'XX', 2 aromatic H *ortho* to OCH₂), 7.98 (AA'XX', 2 aromatic H *ortho* to CO₂). Anal. Calcd for C₁₇H₂₁F₅O₃: C, 55.43; H, 5.75. Found: C, 55.52; H, 5.64.

Ethyl 4-(*n*-Pentafluoroethyl)octyloxy)benzoate. Mp = 43 °C. ¹H NMR: 1.38 (m, CH₃CH₂O₂C and (CH₂)₃CH₂CH₂CF₂), 1.46 (m, CH₂CH₂CH₂O), 1.59 (m, CH₂CH₂CF₂), 1.80 (m, CH₂CH₂O), 2.01 (m, CH₂CF₂), 4.00 (t, *J* = 6.5 Hz, OCH₂), 4.34 (q, *J* = 7.1 Hz, CH₂O₂C), 6.89 (AA'XX', 2 aromatic H *ortho* to OCH₂), 7.98 (AA'XX', 2 aromatic H *ortho* to CO₂). Anal. Calcd for C₁₉H₂₅F₅O₃: C, 57.57; H, 6.36. Found: C, 57.57; H, 6.50.

4-(*n*-Alkenyloxy)benzoic Acids (*n* = 3–6, 8) and 4-(*n*-Perfluoroalkyl)alkoxy)benzoic Acids (*n* = 3–6, 8; *m* = 2). 4-(*n*-Prop-2'-enyloxy)benzoic acid and the 4-(*n*-perfluoroalkyl)alkoxy)benzoic acids were prepared in 73–94% yield as described previously for the 4-(*n*-alkenyloxy)benzoic acids⁴ with *n* = 4–6, 8. For example, ethyl 4-(*n*-prop-2'-enyloxy)benzoate (6.2 g, 30 mmol) and sodium hydroxide (2.4 g, 61 mmol) in ethanol (50 mL) and water (50 mL) were refluxed overnight. After cooling to room temperature, the solution was acidified to a pH of 2 with concentrated HCl. The resulting precipitate was collected and recrystallized from ethanol (135 mL) to yield 4.4 g (82%) of 4-(*n*-prop-2'-enyloxy)benzoic acid as white crystals. ¹H NMR: 4.62 (dt, *J* = 5.3, 1.5 Hz, OCH₂), 5.33 (dq, *J* = 10.5, 1.4 Hz, *E*-HCH=CH), 5.44 (dq, *J* = 17.3, 1.6 Hz, *Z*-HCH=CH), 6.06 (ddt, *J* = 17.3, 10.5, 5.3 Hz, CH=CH₂), 6.96 (AA'XX', 2 aromatic H *ortho* to OCH₂), 8.06 (AA'XX', 2 aromatic H *ortho* to CO₂). Anal. Calcd for C₁₀H₁₀O₃: C, 67.41; H, 5.66. Found: C, 67.49; H, 5.81.

4-(*n*-Pentafluoroethyl)propoxy)benzoic Acid. ¹H NMR: 2.14 (m, CH₂CH₂CF₂), 2.28 (m, CH₂CF₂), 4.11 (t, *J* = 5.9 Hz, OCH₂), 6.94 (d, *J* = 8.9 Hz, 2 aromatic H *ortho* to OCH₂), 8.07 (d, *J* = 8.9 Hz, 2 aromatic H *ortho* to CO₂). Anal. Calcd for C₁₂H₁₁F₅O₃: C, 48.33; H, 3.72. Found: C, 48.23; H, 3.73.

4-(*n*-Pentafluoroethyl)butoxy)benzoic Acid. ¹H NMR: 1.83 (m, CH₂CH₂CF₂), 1.90 (m, CH₂CH₂O), 2.13 (m, CH₂CF₂), 4.07 (t, *J* = 5.9 Hz, OCH₂), 6.90 (d, *J* = 8.8 Hz, 2 aromatic H *ortho* to OCH₂), 7.99 (d, *J* = 8.9 Hz, 2 aromatic H *ortho* to CO₂). Anal. Calcd for C₁₃H₁₃F₅O₃: C, 50.01, 4.20. Found: C, 49.80; H, 4.36.

4-(*n*-Pentafluoroethyl)pentoxy)benzoic Acid. ¹H NMR: 1.61 (m, CH₂CH₂CH₂CF₂), 1.68 (m, CH₂CH₂CF₂), 1.86 (m, CH₂CH₂O), 2.07 (m, CH₂CF₂), 4.05 (t, *J* = 6.3 Hz, OCH₂), 6.92 (d, *J* = 8.8 Hz, 2 aromatic H *ortho* to OCH₂), 8.05 (d, *J* = 8.7 Hz, 2 aromatic H *ortho* to CO₂). Anal. Calcd for C₁₄H₁₅F₅O₃: C, 51.54; H, 4.63. Found: C, 51.38; H, 4.51.

4-(*n*-Pentafluoroethyl)hexoxy)benzoic Acid. ¹H NMR: 1.50 (m, (CH₂)₂CH₂CH₂CF₂), 1.64 (m, CH₂CH₂CF₂), 1.84 (m, CH₂CH₂O), 2.04 (m, CH₂CF₂), 4.04 (t, *J* = 6.2 Hz, OCH₂), 6.93 (d, *J* = 8.7 Hz, 2 aromatic H *ortho* to OCH₂), 8.06 (d, *J* = 8.9 Hz, 2 aromatic H *ortho* to CO₂). Anal. Calcd for C₁₅H₁₇F₅O₃: C, 52.94; H, 5.04. Found: C, 53.07; H, 5.20.

4-(*n*-Pentafluoroethyl)octyloxy)benzoic Acid. ¹H NMR: 1.38 (m, (CH₂)₃CH₂CH₂CF₂), 1.48 (m, CH₂CH₂CH₂O), 1.59 (m, CH₂CH₂CF₂), 1.81 (m, CH₂CH₂O), 2.01 (m, CH₂CF₂), 4.02 (t, *J* = 6.5 Hz, OCH₂), 6.93 (d, *J* = 8.9 Hz, 2 aromatic H *ortho* to OCH₂), 8.05 (d, *J* = 8.9 Hz, 2 aromatic H *ortho* to CO₂). Anal. Calcd for C₁₇H₂₁F₅O₃: C, 55.43; H, 5.75. Found: C, 55.42; H, 6.00.

2,5-Bis[(4'-(*n*-alkenyloxy)benzoyl)oxy]toluenes (*n* = 3–6, 8) and 2,5-Bis[(4'-(*n*-perfluoroalkyl)alkoxy)benzoyl)oxy]toluenes (*n* = 3–6, 8; *m* = 2). 2,5-Bis[(4'-(*n*-prop-2'-enyloxy)benzoyl)oxy]toluene and the 2,5-bis[(4'-(*n*-perfluoroalkyl)alkoxy)benzoyl)oxy]toluenes were prepared in 84–95% yield as described previously for the 2,5-bis[(4'-(*n*-alkenyloxy)benzoyl)oxy]toluenes⁴ with *n* = 4–6, 8.

2,5-Bis[(4'-(*n*-prop-2'-enyloxy)benzoyl)oxy]toluene. ¹H NMR: 2.25 (s, ArCH₃), 4.64 (m, CH₂CH=, 4 H), 5.35 (m, *E*-HCH=CH, 2 H), 5.45 (m, *Z*-HCH=CH, 2 H), 6.08 (m, CH=CH₂, 2 H), 7.00 (m, 4 aromatic H *ortho* to OCH₂), 7.08 (dd, *J* = 8.6, 2.8 Hz, 1 aromatic H *para* to CH₃), 7.13 (d, *J* = 2.7 Hz, 1 aromatic H *ortho* to CH₃), 7.17 (d, *J* = 8.6 Hz, 1 aromatic H *meta* to CH₃), 8.15 (m, 4 aromatic H *ortho* to CO₂). Anal. Calcd for C₂₇H₂₄O₆: C, 72.96; H, 5.44. Found: C, 73.22; H, 5.63.

2,5-Bis[(4'-(*n*-pentafluoroethyl)propoxy)benzoyl)oxy]toluene. ¹H NMR: 2.15 (m, CH₂CH₂CF₂, 4 H), 2.25 (s, ArCH₃), 2.31 (m, CH₂CF₂, 4 H), 4.14 (m, OCH₂, 4 H), 6.99 (m, 4 aromatic H *ortho* to OCH₂), 7.09 (dd, *J* = 8.6, 2.7 Hz, 1 aromatic H *para* to CH₃), 7.13 (d, *J* = 2.9 Hz, 1 aromatic H *ortho* to CH₃), 7.18 (d, *J* = 8.7 Hz, 1 aromatic H *meta* to CH₃), 8.17 (m, 4 aromatic H *ortho* to CO₂). Anal. Calcd for C₃₁H₂₆F₁₀O₆: C, 54.39; H, 3.83. Found: C, 54.40; H, 3.81.

2,5-Bis[(4'-(*n*-pentafluoroethyl)butoxy)benzoyl)oxy]toluene. ¹H NMR: 1.84 (m, CH₂CH₂CF₂, 4 H), 1.92 (m,

$\text{CH}_2\text{CH}_2\text{O}$, 4 H), 2.14 (m, CH_2CF_2 , 4 H), 2.25 (s, ArCH_3), 4.09 (m, OCH_2 , 4 H), 6.98 (m, 4 aromatic H *ortho* to OCH_2), 7.08 (dd, $J = 8.5$, 2.8 Hz, 1 aromatic H *para* to CH_3), 7.13 (d, $J = 2.7$ Hz, 1 aromatic H *ortho* to CH_3), 7.18 (d, $J = 8.7$ Hz, 1 aromatic H *meta* to CH_3), 8.16 (m, 4 aromatic H *ortho* to CO_2). Anal. Calcd for $\text{C}_{33}\text{H}_{30}\text{F}_{10}\text{O}_6$: C, 55.62; H, 4.24. Found: C, 55.72; H, 4.28.

2,5-Bis[(4'-(*n*-pentafluoroethyl)pentoxy)benzoyl]oxy-toluene. ^1H NMR: 1.63 (m, $\text{CH}_2\text{CH}_2\text{CH}_2\text{CF}_2$, 4 H), 1.71 (m, $\text{CH}_2\text{CH}_2\text{CF}_2$, 4 H), 1.88 (m, $\text{CH}_2\text{CH}_2\text{O}$, 4 H), 2.08 (m, CH_2CF_2 , 4 H), 2.24 (s, ArCH_3), 4.07 (m, OCH_2 , 4 H), 6.98 (m, 4 aromatic H *ortho* to OCH_2), 7.08 (dd, $J = 8.7$, 2.6 Hz, 1 aromatic H *para* to CH_3), 7.13 (d, $J = 2.4$ Hz, 1 aromatic H *ortho* to CH_3), 7.18 (d, $J = 8.6$ Hz, 1 aromatic H *meta* to CH_3), 8.16 (m, 4 aromatic H *ortho* to CO_2). Anal. Calcd for $\text{C}_{35}\text{H}_{34}\text{F}_{10}\text{O}_6$: C, 56.76; H, 4.63. Found: C, 56.88; H, 4.89.

2,5-Bis[(4'-(*n*-pentafluoroethyl)hexoxy)benzoyl]oxy-toluene. ^1H NMR: 1.63 (m, $\text{CH}_2\text{CH}_2\text{CH}_2\text{CF}_2$, 4 H), 1.71 (m, $\text{CH}_2\text{CH}_2\text{CF}_2$, 4 H), 1.88 (m, $\text{CH}_2\text{CH}_2\text{O}$, 4 H), 2.04 (m, CH_2CF_2 , 4 H), 2.24 (s, ArCH_3), 4.07 (m, OCH_2 , 4 H), 6.98 (m, 4 aromatic H *ortho* to OCH_2), 7.08 (dd, $J = 8.7$, 2.8 Hz, 1 aromatic H *para* to CH_3), 7.13 (d, $J = 2.7$ Hz, 1 aromatic H *ortho* to CH_3), 7.18 (d, $J = 8.7$ Hz, 1 aromatic H *meta* to CH_3), 8.16 (m, 4 aromatic H *ortho* to CO_2). Anal. Calcd for $\text{C}_{37}\text{H}_{38}\text{F}_{10}\text{O}_6$: C, 57.81; H, 4.98. Found: C, 57.85; H, 4.96.

2,5-Bis[(4'-(*n*-pentafluoroethyl)octyloxy)benzoyl]oxy-toluene. ^1H NMR: 1.39 (m, $(\text{CH}_2)_3\text{CH}_2\text{CH}_2\text{CF}_2$, 12 H), 1.49 (m, $\text{CH}_2\text{CH}_2\text{CH}_2\text{O}$, 4 H), 1.60 (m, $\text{CH}_2\text{CH}_2\text{CF}_2$, 4 H), 1.83 (m, $\text{CH}_2\text{CH}_2\text{O}$, 4 H), 2.02 (m, CH_2CF_2 , 4 H), 2.24 (s, ArCH_3), 4.05 (m, OCH_2 , 4 H), 6.97 (m, 4 aromatic H *ortho* to OCH_2), 7.08 (dd, $J = 8.6$, 2.6 Hz, 1 aromatic H *para* to CH_3), 7.13 (d, $J = 2.6$ Hz, 1 aromatic H *ortho* to CH_3), 7.17 (d, $J = 8.6$ Hz, 1 aromatic H *meta* to CH_3), 8.15 (m, 4 aromatic H *ortho* to CO_2). Anal. Calcd for $\text{C}_{41}\text{H}_{46}\text{F}_{10}\text{O}_6$: C, 59.71; H, 5.62. Found: C, 59.60; H, 5.88.

2,5-Bis[(4'-(*n*-perfluoroalkyl)alkoxy)benzoyl]oxy-toluenes ($n = 3-6$, 8 ; $m = 3-4$). The 2,5-bis[(4'-(*n*-perfluoroalkyl)alkoxy)benzoyl]oxytoluenes were prepared in 46-80% yield as in the following example. 2,5-Bis[(4'-(*n*-prop-2'-enyloxy)benzoyl]oxytoluene (2.1 g, 4.8 mmol), heptafluoropropyl iodide (2.3 mL, 16 mmol), AIBN (0.28 g, 1.7 mmol) and dry toluene (1.4 mL) were combined in a Schlenk flask, which was then sealed with a rubber septum. The solution was degassed by several freeze-pump-thaw cycles and then filled with N_2 and heated at 70 °C for 16 h. This process was repeated until ^1H NMR demonstrated that greater than 90% of the olefin had been consumed. AIBN (0.28 g, 1.7 mmol), tributyltin hydride (4.6 mL, 17 mmol) and dry toluene (10 mL) were then added to the flask and the reaction was heated under N_2 at 70 °C for 2 h. After ^1H NMR demonstrated that the reduction was complete, the reaction was poured into cold hexanes (50 mL) and the precipitate was collected. The precipitate was then purified by column chromatography using silica gel as the stationary phase and CH_2Cl_2 /hexanes/petroleum ether (5:2:1) as the eluent. The solvent was removed by rotary evaporation and the resulting solid was recrystallized from ethanol (60 mL) and toluene (5 mL) to yield 1.7 g (46%) of 2,5-bis[(4'-(*n*-perfluoropropyl)propoxy)benzoyl]oxytoluene as white crystals. The ^1H NMR spectra of the 2,5-bis[(4'-(*n*-perfluoroalkyl)propoxy)benzoyl]oxytoluenes with $m = 3-4$ are identical: 2.17 (m, $\text{CH}_2\text{CH}_2\text{CF}_2$, 4 H), 2.25 (s, ArCH_3), 2.32 (m, CH_2CF_2 , 4 H), 4.14 (m, OCH_2 , 4 H), 6.99 (m, 4 aromatic H *ortho* to OCH_2), 7.09 (dd, $J = 8.6$, 2.9 Hz, 1 aromatic H *para* to CH_3), 7.13 (d, $J = 2.7$ Hz, 1 aromatic H *ortho* to CH_3), 7.18 (d, $J = 8.6$ Hz, 1 aromatic H *meta* to CH_3), 8.17 (m, 4 aromatic H *ortho* to CO_2). Anal. Calcd for $\text{C}_{33}\text{H}_{26}\text{F}_{14}\text{O}_6$: C, 50.52; H, 3.34. Found: C, 50.38; H, 3.53. Anal. Calcd for $\text{C}_{35}\text{H}_{26}\text{F}_{18}\text{O}_6$: C, 47.53; H, 2.96. Found: C, 47.46; H, 3.17.

The ^1H NMR spectra of the 2,5-bis[(4'-(*n*-perfluoroalkyl)butoxy)benzoyl]oxytoluenes with $m = 3-4$ are identical: 1.86 (m, $\text{CH}_2\text{CH}_2\text{CF}_2$, 4 H), 1.93 (m, $\text{CH}_2\text{CH}_2\text{O}$, 4 H), 2.15 (m, CH_2CF_2 , 4 H), 2.24 (s, ArCH_3), 4.09 (m, OCH_2 , 4 H), 6.98 (m, 4 aromatic H *ortho* to OCH_2), 7.08 (dd, $J = 8.4$, 2.7 Hz, 1 aromatic H *para* to CH_3), 7.13 (d, $J = 2.7$ Hz, 1 aromatic H *ortho* to CH_3), 7.18 (d, $J = 8.7$ Hz, 1 aromatic H *meta* to CH_3),

8.16 (m, 4 aromatic H *ortho* to CO_2). Anal. Calcd for $\text{C}_{35}\text{H}_{30}\text{F}_{14}\text{O}_6$: C, 51.73; H, 3.72. Found: C, 51.84; H, 3.84. Anal. Calcd for $\text{C}_{37}\text{H}_{30}\text{F}_{18}\text{O}_6$: C, 48.70; H, 3.31. Found: C, 48.85; H, 3.48.

The ^1H NMR spectra of the 2,5-bis[(4'-(*n*-perfluoroalkyl)pentoxy)benzoyl]oxytoluenes with $m = 3-4$ are identical: 1.62 (m, $\text{CH}_2\text{CH}_2\text{CH}_2\text{CF}_2$, 4 H), 1.71 (m, $\text{CH}_2\text{CH}_2\text{CF}_2$, 4 H), 1.88 (m, $\text{CH}_2\text{CH}_2\text{O}$, 4 H), 2.11 (m, CH_2CF_2 , 4 H), 2.24 (s, ArCH_3), 4.07 (m, OCH_2 , 4 H), 6.97 (m, 4 aromatic H *ortho* to OCH_2), 7.08 (dd, $J = 8.6$, 2.8 Hz, 1 aromatic H *para* to CH_3), 7.13 (d, $J = 2.5$ Hz, 1 aromatic H *ortho* to CH_3), 7.18 (d, $J = 8.7$ Hz, 1 aromatic H *meta* to CH_3), 8.16 (m, 4 aromatic H *ortho* to CO_2). Anal. Calcd for $\text{C}_{37}\text{H}_{34}\text{F}_{14}\text{O}_6$: C, 52.86; H, 4.08. Found: C, 52.95; H, 4.11. Anal. Calcd for $\text{C}_{39}\text{H}_{34}\text{F}_{18}\text{O}_6$: C, 49.80; H, 3.64. Found: C, 49.77; H, 3.88.

The ^1H NMR spectra of the 2,5-bis[(4'-(*n*-perfluoroalkyl)hexoxy)benzoyl]oxytoluenes with $m = 3-4$ are identical: 1.52 (m, $(\text{CH}_2)_2\text{CH}_2\text{CH}_2\text{CF}_2$, 8 H), 1.66 (m, $\text{CH}_2\text{CH}_2\text{CF}_2$, 4 H), 1.86 (m, $\text{CH}_2\text{CH}_2\text{O}$, 4 H), 2.07 (m, CH_2CF_2 , 4 H), 2.24 (s, ArCH_3), 4.06 (m, OCH_2 , 4 H), 6.98 (m, 4 aromatic H *ortho* to OCH_2), 7.08 (dd, $J = 8.8$, 2.5 Hz, 1 aromatic H *para* to CH_3), 7.13 (d, $J = 2.5$ Hz, 1 aromatic H *ortho* to CH_3), 7.18 (d, $J = 8.7$ Hz, 1 aromatic H *meta* to CH_3), 8.16 (m, 4 aromatic H *ortho* to CO_2). Anal. Calcd for $\text{C}_{39}\text{H}_{38}\text{F}_{14}\text{O}_6$: C, 53.92, 4.41. Found: C, 53.70; H, 4.56. Anal. Calcd for $\text{C}_{41}\text{H}_{38}\text{F}_{18}\text{O}_6$: C, 50.84; H, 3.95. Found: C, 50.86; H, 3.99.

The ^1H NMR spectra of the 2,5-bis[(4'-(*n*-perfluoroalkyl)octyloxy)benzoyl]oxytoluenes with $m = 3-4$ are identical: 1.39 (m, $(\text{CH}_2)_3\text{CH}_2\text{CH}_2\text{CF}_2$, 12 H), 1.50 (m, $\text{CH}_2\text{CH}_2\text{CH}_2\text{O}$, 4 H), 1.62 (m, $\text{CH}_2\text{CH}_2\text{CF}_2$, 4 H), 1.83 (m, $\text{CH}_2\text{CH}_2\text{O}$, 4 H), 2.04 (m, CH_2CF_2 , 4 H), 2.24 (s, ArCH_3), 4.05 (m, OCH_2 , 4 H), 6.97 (m, 4 aromatic H *ortho* to OCH_2), 7.08 (dd, $J = 8.6$, 2.6 Hz, 1 aromatic H *para* to CH_3), 7.13 (d, $J = 2.7$ Hz, 1 aromatic H *ortho* to CH_3), 7.17 (d, $J = 8.6$ Hz, 1 aromatic H *meta* to CH_3), 8.15 (m, 4 aromatic H *ortho* to CO_2). Anal. Calcd for $\text{C}_{43}\text{H}_{46}\text{F}_{14}\text{O}_6$: C, 55.85; H, 5.01. Found: C, 55.74; H, 5.08. Anal. Calcd for $\text{C}_{45}\text{H}_{46}\text{F}_{18}\text{O}_6$: C, 52.74; H, 4.52. Found: C, 52.53; H, 4.63.

2,5-Bis[(4'-(*n*-perfluoroalkyl)alkoxy)benzoyl]oxy-benzyl bromides ($n = 3-6$, 8 ; $m = 2-4$). The 2,5-bis[(4'-(*n*-perfluoroalkyl)alkoxy)benzoyl]oxybenzyl bromides were prepared in 41-70% yield as in the following example. A solution of 2,5-bis[(4'-(*n*-pentafluoroethyl)propoxy)benzoyl]oxytoluene (1.6 g, 2.3 mmol), AIBN (21 mg, 0.13 mmol) and NBS (0.74 g, 4.2 mmol) in benzene (14 mL) was heated at reflux for 4 h. The resulting orange mixture was then poured immediately into 5% aq sodium bisulfite (40 mL) in a separatory funnel. The organic layer was collected and the solvent was removed by rotary evaporation. The residue was dissolved in a minimal amount of CH_2Cl_2 (3 mL) and precipitated in cold methanol (100 mL). The precipitate was collected and dried in vacuo to yield 1.2 g (68%) of a white solid containing 60% 2,5-bis[(4'-(*n*-pentafluoroethyl)propoxy)benzoyl]oxybenzyl bromide (41% overall yield), 6% unreacted 2,5-bis[(4'-(*n*-pentafluoroethyl)propoxy)benzoyl]oxytoluene, and 34% 2,5-bis[(4'-(*n*-pentafluoroethyl)propoxy)benzoyl]oxybenzyl dibromide. This crude product was used without further purification. The ^1H NMR spectra of the 2,5-bis[(4'-(*n*-perfluoroalkyl)propoxy)benzoyl]oxybenzyl bromides with $m = 2-4$ are identical: 2.17 (m, $\text{CH}_2\text{CH}_2\text{CF}_2$, 4 H), 2.33 (m, CH_2CF_2 , 4 H), 4.15 (m, OCH_2 , 4 H), 4.45 (s, ArCH_2Br), 7.00 (m, 4 aromatic H *ortho* to OCH_2), 7.29 (m, 3 aromatic H of central ring), 8.19 (m, 4 aromatic H *ortho* to CO_2).

The ^1H NMR spectra of the 2,5-bis[(4'-(*n*-perfluoroalkyl)butoxy)benzoyl]oxybenzyl bromides with $m = 2-4$ are identical: 1.86 (m, $\text{CH}_2\text{CH}_2\text{CF}_2$, 4 H), 1.93 (m, $\text{CH}_2\text{CH}_2\text{O}$, 4 H), 2.18 (m, CH_2CF_2 , 4 H), 4.10 (m, OCH_2 , 4 H), 4.45 (s, ArCH_2Br), 6.99 (d, 4 aromatic H *ortho* to OCH_2), 7.29 (m, 3 aromatic H of central ring), 8.18 (d, 4 aromatic H *ortho* to CO_2).

The ^1H NMR spectra of the 2,5-bis[(4'-(*n*-perfluoroalkyl)pentoxy)benzoyl]oxybenzyl bromides with $m = 2-4$ are identical: 1.62 (m, $\text{CH}_2\text{CH}_2\text{CH}_2\text{CF}_2$, 4 H), 1.69 (m, $\text{CH}_2\text{CH}_2\text{CF}_2$, 4 H), 1.89 (m, $\text{CH}_2\text{CH}_2\text{O}$, 4 H), 2.11 (m, CH_2CF_2 , 4 H), 4.07 (m, OCH_2 , 4 H), 4.45 (s, ArCH_2Br), 6.99 (m, 4 aromatic H

ortho to OCH₂), 7.29 (m, 3 aromatic H of central ring), 8.18 (m, 4 aromatic H *ortho* to CO₂).

The ¹H NMR spectra of the 2,5-bis[(4'-(*n*-perfluoroalkyl)-hexoxy)benzoyloxy]benzyl bromides with *m* = 2–4 are identical: 1.52 (m, (CH₂)₂CH₂CH₂CF₂, 8 H), 1.66 (m, CH₂CH₂CF₂, 4 H), 1.86 (m, CH₂CH₂O, 4 H), 2.08 (m, CH₂CF₂, 4 H), 4.07 (m, OCH₂, 4 H), 4.45 (s, ArCH₂Br), 6.99 (m, 4 aromatic H *ortho* to OCH₂), 7.29 (m, 3 aromatic H of central ring), 8.17 (m, 4 aromatic H *ortho* to CO₂).

The ¹H NMR spectra of the 2,5-bis[(4'-(*n*-perfluoroalkyl)-octyloxy)benzoyloxy]benzyl bromides with *m* = 2–4 are identical: 1.39 (m, (CH₂)₃CH₂CH₂CF₂, 12 H), 1.50 (m, CH₂-CH₂CH₂O, 4 H), 1.60 (m, CH₂CH₂CF₂, 4 H), 1.83 (m, CH₂CH₂O, 4 H), 2.02 (m, CH₂CF₂, 4 H), 4.06 (m, OCH₂, 4 H), 4.45 (s, ArCH₂Br), 6.99 (m, 4 aromatic H *ortho* to OCH₂), 7.29 (m, 3 aromatic H of central ring), 8.17 (m, 4 aromatic H *ortho* to CO₂).

In addition to the above resonances, products from this reaction contained singlets at 2.24 ppm (ArCH₃) due to residual starting material, and at 6.8 (ArCHBr₂) and 7.7 ppm (1 aromatic H *ortho* to CHBr₂) due to dibrominated material.

5-[[[2',5'-Bis(4'-(*n*-perfluoroalkyl)alkoxy)benzoyloxy]benzyl]oxy]carbonyl]bicyclo[2.2.1]hept-2-enes (*n* = 3–6, **8; *m* = 2–4; 25–75% endo).** The monomers were prepared in 33–85% yield as in the following example for *n*, *m* = 3, 2. A solution of 2,5-bis[(4'-(*n*-pentafluoroethyl)propoxy)benzoyloxy]benzyl bromide (1.2 g, 0.93 mmol ArCH₂Br), TBAH (46 mg, 0.13 mmol), potassium bicyclo[2.2.1]hept-2-ene-5-carboxylate (0.23 g, 1.3 mmol) and dry DMSO (0.70 mL) in dry THF (7.0 mL) was heated at 60 °C for 22 h. The reaction mixture was poured into cold water (100 mL) and extracted twice with CH₂Cl₂ (100 mL total). The combined organic layers were passed through a short column of basic activated alumina using CH₂Cl₂ as the eluent. The solvent was removed by rotary evaporation and the residue was purified by column chromatography using silica gel as the stationary phase and a gradient of CH₂Cl₂/hexanes as the eluent. The solvent was removed by rotary evaporation and the residue was recrystallized from ethanol (35 mL) and toluene (1 mL) to yield 0.57 g (75%) of 5-[[[2',5'-bis(4'-(*n*-pentafluoroethyl)propoxy)benzoyloxy]benzyl]oxy]carbonyl]bicyclo[2.2.1]hept-2-ene as a white solid. Before polymerization, the monomer was recrystallized in a drybox from dry hexanes (12 mL) and toluene (9 mL); yield, 0.47 g (62%). The ¹H NMR spectra of the 5-[[[2',5'-bis(4'-(*n*-perfluoroalkyl)propoxy)benzoyloxy]benzyl]oxy]carbonyl]bicyclo[2.2.1]hept-2-enes with *m* = 2–4 are identical: 1.31 (m, *endo* norbornyl 6- and 7-CH₂), 1.83 (m, *exo* norbornyl 6-CH₂), 2.17 (m, CH₂CH₂CF₂ and *exo* norbornyl 5-CH), 2.33 (m, CH₂CF₂, 4 H), 2.86 (m, *endo* norbornyl 1-CH), 2.89 (m, *exo* norbornyl 4-CH), 2.92 (m, *endo* norbornyl 5-CH), 2.95 (m, *exo* norbornyl 1-CH), 3.14 (m, *endo* norbornyl 4-CH), 4.15 (t, *J* = 5.9 Hz, OCH₂, 4 H), 5.09 (AB, *endo* ArCH₂O), 5.15 (s, *exo* ArCH₂O), 5.80 (m, *endo* norbornyl 2-CH), 6.04 (m, *exo* norbornyl 2-CH), 6.10 (m, norbornyl 3-CH), 6.99 (m, 4 aromatic H *ortho* to OCH₂), 7.29 (m, 3 aromatic H of central ring), 8.16 (m, 4 aromatic H *ortho* to CO₂). Anal. Calcd for *n*, *m* = 3, 2, C₃₉H₃₄F₁₀O₈, 67% endo: C, 57.08; H, 4.18. Found: C, 56.99; H, 4.23. Anal. Calcd for *n*, *m* = 3, 3, C₄₁H₃₄F₁₄O₈, 59% endo: C, 53.49; H, 3.72. Found: C, 53.34; H, 3.85. Anal. Calcd for *n*, *m* = 3, 4, C₄₃H₃₄F₁₈O₈, 65% endo: C, 50.60; H, 3.36. Found: C, 50.56; H, 3.52.

The ¹H NMR spectra of the 5-[[[2',5'-bis(4'-(*n*-perfluoroalkyl)butoxy)benzoyloxy]benzyl]oxy]carbonyl]bicyclo[2.2.1]hept-2-enes with *m* = 2–4 are identical: 1.31 (m, *endo* norbornyl 6- and 7-CH₂), 1.85 (m, CH₂CH₂CF₂ and *exo* norbornyl 6-CH₂), 1.93 (m, CH₂CH₂O, 4 H), 2.18 (m, CH₂CF₂ and *exo* norbornyl 5-CH), 2.86 (m, *endo* norbornyl 1-CH), 2.89 (m, *exo* norbornyl 4-CH), 2.92 (m, *endo* norbornyl 5-CH), 2.95 (m, *exo* norbornyl 1-CH), 3.14 (m, *endo* norbornyl 4-CH), 4.10 (t, *J* = 5.5 Hz, OCH₂, 4 H), 5.08 (AB, *endo* ArCH₂O), 5.15 (s, *exo* ArCH₂O), 5.80 (m, *endo* norbornyl 2-CH), 6.04 (m, *exo* norbornyl 2-CH), 6.10 (m, norbornyl 3-CH), 6.98 (m, 4 aromatic H *ortho* to OCH₂), 7.28 (m, 3 aromatic H of central ring), 8.15 (m, 4 aromatic H *ortho* to CO₂). Anal. Calcd for *n*, *m* = 4, 2, C₄₁H₃₈F₁₀O₈, 75% endo: C, 58.02; H, 4.51. Found: C, 57.83;

H, 4.59. Anal. Calcd for *n*, *m* = 4, 3, C₄₃H₃₈F₁₄O₈, 31% endo: C, 54.44; H, 4.04. Found: C, 54.75; H, 4.21. Anal. Calcd for *n*, *m* = 4, 4, C₄₅H₃₈F₁₈O₈, 67% endo: C, 51.54; H, 3.65. Found: C, 51.08; H, 3.72.

The ¹H NMR spectra of the 5-[[[2',5'-bis(4'-(*n*-perfluoroalkyl)pentoxy)benzoyloxy]benzyl]oxy]carbonyl]bicyclo[2.2.1]hept-2-enes with *m* = 2–4 are identical: 1.31 (m, *endo* norbornyl 6- and 7-CH₂), 1.62 (m, CH₂CH₂CF₂, 4 H), 1.71 (m, CH₂CH₂CF₂, 4 H), 1.88 (m, CH₂CH₂O and *exo* norbornyl 6-CH₂), 2.10 (m, CH₂CF₂ and *exo* norbornyl 5-CH), 2.86 (m, *endo* norbornyl 1-CH), 2.89 (m, *exo* norbornyl 4-CH), 2.92 (m, *endo* norbornyl 5-CH), 2.95 (m, *exo* norbornyl 1-CH), 3.14 (m, *endo* norbornyl 4-CH), 4.07 (t, *J* = 6.2 Hz, OCH₂, 4 H), 5.08 (AB, *endo* ArCH₂O), 5.15 (s, *exo* ArCH₂O), 5.80 (m, *endo* norbornyl 2-CH), 6.04 (m, *exo* norbornyl 2-CH), 6.10 (m, norbornyl 3-CH), 6.98 (m, 4 aromatic H *ortho* to OCH₂), 7.27 (m, 3 aromatic H of central ring), 8.15 (m, 4 aromatic H *ortho* to CO₂). Anal. Calcd for *n*, *m* = 5, 2, C₄₃H₄₂F₁₀O₈, 62% endo: C, 58.90; H, 4.83. Found: C, 58.82; H, 4.91. Anal. Calcd for *n*, *m* = 5, 3, C₄₅H₄₂F₁₄O₈, 57% endo: C, 55.33; H, 4.33. Found: C, 55.28; H, 4.48. Anal. Calcd for *n*, *m* = 5, 4, C₄₇H₄₂F₁₈O₈, 73% endo: C, 52.42; H, 3.93. Found: C, 52.33; H, 4.09.

The ¹H NMR spectra of the 5-[[[2',5'-bis(4'-(*n*-perfluoroalkyl)hexoxy)benzoyloxy]benzyl]oxy]carbonyl]bicyclo[2.2.1]hept-2-enes with *m* = 2–4 are identical: 1.31 (m, *endo* norbornyl 6- and 7-CH₂), 1.52 (m, (CH₂)₂CH₂CH₂CF₂, 8 H), 1.65 (m, CH₂CH₂CF₂, 4 H), 1.84 (m, CH₂CH₂O and *exo* norbornyl 6-CH₂), 2.08 (m, CH₂CF₂ and *exo* norbornyl 5-CH), 2.85 (m, *endo* norbornyl 1-CH), 2.89 (m, *exo* norbornyl 4-CH), 2.91 (m, *endo* norbornyl 5-CH), 2.95 (m, *exo* norbornyl 1-CH), 3.14 (m, *endo* norbornyl 4-CH), 4.06 (t, *J* = 6.3 Hz, OCH₂, 4 H), 5.08 (AB, *endo* ArCH₂O), 5.15 (s, *exo* ArCH₂O), 5.80 (m, *endo* norbornyl 2-CH), 6.04 (m, *exo* norbornyl 2-CH), 6.10 (m, norbornyl 3-CH), 6.98 (m, 4 aromatic H *ortho* to OCH₂), 7.28 (m, 3 aromatic H of central ring), 8.15 (m, 4 aromatic H *ortho* to CO₂). Anal. Calcd for *n*, *m* = 6, 2, C₄₅H₄₆F₁₀O₈, 67% endo: C, 59.73; H, 5.12. Found: C, 59.78; H, 5.16. Anal. Calcd for *n*, *m* = 6, 3, C₄₇H₄₆F₁₄O₈, 75% endo: C, 56.18; H, 4.61. Found: C, 55.88; H, 4.69. Anal. Calcd for *n*, *m* = 6, 4, C₄₉H₄₆F₁₈O₈, 45% endo: C, 53.27; H, 4.20. Found: C, 53.17; H, 4.41.

The ¹H NMR spectra of the 5-[[[2',5'-bis(4'-(*n*-perfluoroalkyl)octyloxy)benzoyloxy]benzyl]oxy]carbonyl]bicyclo[2.2.1]hept-2-enes with *m* = 2–4 are identical: 1.31 (m, *endo* norbornyl 6- and 7-CH₂), 1.39 (m, (CH₂)₃CH₂CH₂CF₂, 12 H), 1.50 (m, CH₂CH₂CH₂O, 4 H), 1.58 (m, CH₂CH₂CF₂, 4 H), 1.83 (m, CH₂CH₂O and *exo* norbornyl 6-CH₂), 2.02 (m, CH₂CF₂, 4 H), 2.17 (m, *exo* norbornyl 5-CH), 2.85 (m, *endo* norbornyl 1-CH), 2.89 (m, *exo* norbornyl 4-CH), 2.91 (m, *endo* norbornyl 5-CH), 2.95 (m, *exo* norbornyl 1-CH), 3.14 (m, *endo* norbornyl 4-CH), 4.05 (t, *J* = 6.3 Hz, OCH₂, 4 H), 5.08 (AB, *endo* ArCH₂O), 5.15 (s, *exo* ArCH₂O), 5.80 (m, *endo* norbornyl 2-CH), 6.04 (m, *exo* norbornyl 2-CH), 6.10 (m, norbornyl 3-CH), 6.98 (d, 4 aromatic H *ortho* to OCH₂), 7.28 (m, 3 aromatic H of central ring), 8.14 (d, 4 aromatic H *ortho* to CO₂). Anal. Calcd for *n*, *m* = 8, 2, C₄₉H₅₄F₁₀O₈, 67% endo: C, 61.25, 5.66. Found: C, 61.21; H, 5.50. Anal. Calcd for *n*, *m* = 8, 3, C₅₁H₅₄F₁₄O₈, 25% endo: C, 57.74; H, 5.13. Found: C, 57.48; H, 5.19. Anal. Calcd for *n*, *m* = 8, 4, C₅₃H₅₄F₁₈O₈, 31% endo: C, 54.83; H, 4.69. Found: C, 54.39; H, 4.78.

Poly{5-[[[2',5'-bis(4'-(*n*-perfluoroalkyl)alkoxy)benzoyloxy]benzyl]oxy]carbonyl]bicyclo[2.2.1]hept-2-ene}s (*n* = 3–6, **8; *m* = 2–4).** The polynorbornenes were prepared in 18–92% yield as in the following example. In a drybox, a solution of 5-[[[2',5'-bis(4'-(*n*-pentafluoroethyl)propoxy)benzoyloxy]benzyl]oxy]carbonyl]bicyclo[2.2.1]hept-2-ene (0.30 g, 0.36 mmol) in degassed THF (9.5 g) was added dropwise over 3 min to a solution of Mo(CHCMe₂Ph)(N-2,6-*i*-Pr₂Ph)(O*t*-Bu)₂ (4 mg, 7 μmol) in THF (0.52 g) at 25 °C. After being stirred at 25 °C for an additional 2 h, benzaldehyde (20 μL, 0.20 mmol) was added and the mixture was stirred for another 30 min. The solution was removed from the drybox and the polymer was precipitated in methanol (70 mL). The precipitate was collected and reprecipitated from THF (14 mL) into methanol (100 mL) to yield 0.26 g (88%) of poly{5-[[[2',5'-bis(4'-(*n*-perfluoroethyl)propoxy)benzoyloxy]benzyl]oxy]-

carbonyl]bicyclo[2.2.1]hept-2-ene} as a white powder; $M_n = 3.24 \times 10^4$, $M_w/M_n = 1.43$.

Acknowledgment. Acknowledgment is made to the donors of the Petroleum Research Fund, administered by the American Chemical Society, for support of this research. C.P. also acknowledges the National Science Foundation for an NSF Young Investigator Award (1994-2000), and matching funds from Goodyear Tire & Rubber Company and A. Schulman, Inc. We also thank Professor Vincent Pecoraro for giving A.C.S. laboratory space during his final two years at the University of Michigan to carry out many of the syntheses described in this paper.

Supporting Information Available: Figure showing a polarized optical micrograph of the nematic schlieren texture of the $n, m = 6, 2$ polymer. This material is available free of charge via the Internet at <http://pubs.acs.org>.

References and Notes

- (1) Demus, D.; Zschke, H. *Flussige Kristalle in Tabellen II*; VEB Deutscher Verlag: Leipzig, Germany, 1984.
- (2) Reinitzer, F. *Monatsch Chem.* **1888**, *9*, 421.
- (3) See for example: (a) Young, W. R.; Green, D. C. *Mol. Cryst. Liq. Cryst.* **1974**, *26*, 7. (b) Weissflog, W.; Schlick, R.; Demus, D. *Z. Chem.* **1981**, *21*, 452. (c) Weissflog, W.; Demus, D. *Cryst. Res. Technol.* **1983**, *18*, K21. (d) Weissflog, W.; Demus, D. *Cryst. Res. Technol.* **1984**, *19*, 55. (e) Weissflog, W.; Demus, D. *Mol. Cryst. Liq. Cryst.* **1985**, *129*, 235. (f) Weissflog, W.; Wiegeleben, A.; Demus, D. *Mater. Chem. Phys.* **1985**, *12*, 461. (g) Ballauff, M. *Liq. Cryst.* **1987**, *2*, 519. (h) Imrie, C. T.; Taylor, L. *Liq. Cryst.* **1989**, *6*, 1. (i) Stützer, C.; Weissflog, W.; Stegemeyer, H. *Liq. Cryst.* **1996**, *21*, 557. (j) Andersch, J.; Tschierske, C. *Liq. Cryst.* **1996**, *21*, 51.
- (4) Arehart, S. V.; Pugh, C. *J. Am. Chem. Soc.* **1997**, *119*, 3027.
- (5) Pugh, C.; Bae, J.-Y.; Dharia, J.; Ge, J. J.; Cheng, S. Z. D. *Macromolecules* **1998**, *31*, 5188.
- (6) (a) Rabolt, J. F.; Russel, T. P.; Tweig, R. J. *Macromolecules* **1984**, *17*, 2786. (b) Mahler, W.; Guillon, D.; Skoulios, A. *Mol. Cryst. Liq. Cryst.* **1985**, *2*, 111. (c) Russel, T. P.; Rabolt, J. F.; Tweig, R. J.; Siemens, R. L.; Farmer, B. L. *Macromolecules* **1986**, *19*, 1135. (d) Höpken, J.; Pugh, C.; Richtering, W.; Möller, M. *Makromol. Chem.* **1988**, *189*, 911. (e) Viney, C.; Russell, T. P.; Depero, L. E.; Tweig, R. J. *Mol. Cryst. Liq. Cryst.* **1989**, *168*, 63. (f) Viney, C.; Tweig, R. J.; Russell, T. P.; Depero, L. E. *Liq. Cryst.* **1989**, *5*, 1783. (g) Viney, C.; Tweig, R. J.; Gordon, B. R.; Rabolt, J. F. *Mol. Cryst. Liq. Cryst.* **1991**, *198*, 285. (h) Höpken, J.; Möller, M. *Macromolecules* **1992**, *25*, 2482.
- (7) (a) Small, A. C.; Hunt, D. K.; Pugh, C. *Liq. Cryst.* **1999**, *26*, 849. (b) Pugh, C.; Small, A. C.; Helfer, C. A.; Mattice, W. L. *Liq. Cryst.* **2001**, *28*, 991.
- (8) (a) Pugh, C.; Dharia, J.; Arehart, S. V. *Macromolecules* **1997**, *30*, 4520. (b) Pugh, C.; Shao, J.; Ge, J. J.; Cheng, S. Z. D. *Macromolecules* **1998**, *31*, 1779. (c) Kim, G.-H.; Pugh, C.; Cheng, S. Z. D. *Macromolecules* **2000**, *33*, 8983.
- (9) (a) Hessel, F.; Finkelmann, H. *Polym. Bull.* **1985**, *14*, 375. (b) Hessel, F.; Herr, R.-P.; Finkelmann, H. *Makromol. Chem.* **1987**, *188*, 1597. (c) Zhou, Q.-F.; Li, H.-M.; Feng, X. D. *Macromolecules* **1987**, *20*, 233. (d) Zhou, Q.-F.; Li, H.-M.; Feng, X. D. *Mol. Cryst. Liq. Cryst.* **1988**, *155*, 73. (e) Keller, P.; Hardouin, F.; Mauzac, M.; Achard, M. F. *Mol. Cryst. Liq. Cryst.* **1988**, *155*, 171. (f) Attard, G. S.; Araki, K.; Moura-Ramos, J. J.; Williams, G. *Liq. Cryst.* **1988**, *3*, 861. (g) Hessel, F.; Finkelmann, H. *Makromol. Chem.* **1988**, *189*, 2275. (h) Hardouin, F.; Mery, S.; Achard, M. F.; Mauzac, M.; Davidson, P.; Keller, P. *Liq. Cryst.* **1990**, *8*, 565. (i) Hardouin, F.; Mery, S.; Achard, M. F.; Noirez, L.; Keller, P. *J. Phys. II Fr.* **1991**, *1*, 511. (j) Hardouin, F.; Leroux, N.; Mery, S.; Noirez, L. *J. Phys. II Fr.* **1992**, *2*, 271. (k) Lewthwaite, R. A.; Gray, G. W.; Toyne, K. J. *J. Mater. Chem.* **1992**, *2*, 119. (l) Percec, V.; Tomazos, D. *J. Mater. Chem.* **1993**, *3*, 643. (m) Leroux, N.; Keller, P.; Achard, M. F.; Noirez, L.; Hardouin, F. *J. Phys. II Fr.* **1993**, *3*, 1289. (n) Cherodian, A. S.; Hughes, N. J.; Richardson, R. M.; Lee, M. S. K.; Gray, G. W. *Liq. Cryst.* **1993**, *14*, 1667. (o) Leroux, N.; Achard, M. F.; Keller, P.; Hardouin, F. *Liq. Cryst.* **1994**, *16*, 1073. (p) Achard, M. F.; Lecommandoux, S.; Hardouin, F. *Liq. Cryst.* **1995**, *19*, 581. (q) Takenaka, S.; Yamasaki, Y. *Mol. Cryst. Liq. Cryst.* **1995**, *258*, 51. (r) Jegou, C.; Leroux, N.; Agricole, B.; Mingotaud, C. *Liq. Cryst.* **1996**, *20*, 691. (s) Leroux, N.; Chien, L.-C. *Liq. Cryst.* **1996**, *21*, 189. (t) Lecommandoux, S.; Achard, M. F.; Hardouin, F.; Bulet, A.; Cotton, J. P. *Liq. Cryst.* **1997**, *22*, 549. (u) Pragliola, S.; Ober, C. K.; Mather, P. T.; Jeon, H. G. *Macromol. Chem. Phys.* **1999**, *200*, 2338. (v) Mi, Q.-D.; Zhou, Q.-F. *Chin. J. Polym. Sci.* **2000**, *18*, 139.
- (10) $n = 1-6$: Pugh, C.; Shrock, R. R. *Macromolecules* **1992**, *25*, 6593.
- (11) (a) Pugh, C.; Kiste, A. L. *Prog. Polym. Sci.* **1997**, *22*, 601. (b) Pugh, C.; Kiste, A. L. In *Handbook of Liquid Crystals*; Demus, D.; Goodby, J. W.; Gray, G. W.; Spiess, H. W., Vill, V., Eds.; VCH: Weinheim, Germany, 1998; Vol. 3, Chapter 3.
- (12) (a) Demus, D.; Richter, L. *Textures of Liquid Crystals*; Verlag Chemie: Weinheim, Germany, 1978. (b) Gray, G. W.; Goodby, J. W. *Smectic Liquid Crystals. Textures and Structures*; Leonard Hill: Glasgow, Scotland, 1984.
- (13) $n = 7-16$: Pugh, C.; Small, A. C. Unpublished results.
- (14) (a) Weissflog, W.; Demus, D. *Cryst. Res. Technol.* **1983**, *18*, K21. (b) Weissflog, W.; Demus, D. *Cryst. Res. Technol.* **1984**, *19*, 55.
- (15) *Polymer Handbook*, 3rd ed.; Brandrup, J., Immergut, E. H., Eds.; Wiley-Interscience: New York, 1989.
- (16) (a) Feast, W. J.; Gibson, V. C.; Khosravi, E.; Marshall, E. L.; Mitchell, J. P. *Polymer* **1992**, *33*, 872. (b) Feast, W. J.; Gibson, V. C.; Marshall, E. L. *J. Chem. Soc., Chem. Commun.* **1992**, 1157.
- (17) Christensen, J. J.; Hanks, R. W.; Izatt, R. M. *Handbook of Heats of Mixing*; Wiley: New York, 1982; p 871.
- (18) (a) Hildebrand, J. H.; Fisher, B. B.; Benesi, H. A. *J. Am. Chem. Soc.* **1950**, *72*, 4348. (b) Young, C. L. *Trans. Faraday Soc.* **1969**, 2639 and references therein.
- (19) (a) Schrock, R. R.; Murdzek, J. S.; Bazan, G. C.; Robbins, J.; DiMare, M.; O'Regan, M. *J. Am. Chem. Soc.* **1990**, *112*, 3875. (b) Fox, H. H.; Yap, K. B.; Robbins, J.; Cai, S.; Schrock, R. R. *Inorg. Chem.* **1992**, *31*, 2287.

MA0113430